NACA RM E53H10

RESEARCH MEMORANDUM

INVESTIGATION OF A 10-STAGE SUBSONIC AXIAL-FLOW RESEARCH COMPRESSOR

V - EFFECT OF REDUCING INLET-GUIDE-VANE TURNING ON OVER-ALL AND INLET-STAGE PERFORMANCE

By Ray E. Budinger and George K. Serovy

Lewis Flight Propulsion Laboratory
Cleveland, Ohio

NATIONAL ADVISORY COMMITTEE
FOR AERONAUTICS

WASHINGTON
March 15, 1954

NACA RM E53H10

NATIONAL ADVISORY COMMITTEE FOR AERONAUTICS

RESEARCH MEMORANDUM

INVESTIGATION OF A 10-STAGE SUBSONIC AXIAL-FLOW RESEARCH COMPRESSOR V - EFFECT OF REDUCING INLET-GUIDE-VANE TURNING ON OVER-ALL AND INLET-STAGE PERFORMANCE

By Ray E. Budinger and George K. Serovy

SUMMARY

The inlet-guide-vane setting of a 10-stage compressor was reduced in order to approximate more closely the design absolute entrance flow angles to the first rotor. In order to determine the effects of the radial redistribution of flow conditions entering the first rotor caused by resetting the guide vanes, the performance of the inlet stage was obtained simultaneously with the over-all compressor performance for both the original and the reduced incidence angles. At the reduced guide-vane setting, only the speeds above the knee in the compressor surge line were noticeably affected. At design speed, the surge pressure ratio increased from 7.52 to 7.66, the maximum equivalent weight flow increased from 56.7 to 58.2 pounds per second, and the peak efficiency increased approximately 1 point, to 0.815. The knee in the compressor surge line occurred at a slightly higher speed at the reduced guide-vane incidence, being initiated at 73-percent design speed compared with 70 percent for the original guide-vane setting. The wall static-pressure-ratio distribution through the compressor indicated that the changes in high-speed compressor performance were due primarily to the increased loading on the first rotor row.

Inlet-guide-vane resetting appears to be a possible means of obtaining design-point operation in an axial-flow compressor. Slight adjustments in guide-vane setting that will permit the inlet stage to operate in a favorable range of angle of attack can be made to compensate for design-efficiency and boundary-layer assumptions. Analysis and experimental data indicate that very large guide-vane adjustments would be required to improve the starting and acceleration characteristics of a jet engine.

INTRODUCTION

The preliminary analysis of the over-all performance of the 10-stage subsonic axial-flow compressor presented in reference 1 indicated that the inlet-stage rotor was operating considerably below its design pressure ratio at design speed. Subsequent surveys of absolute flow angles entering the first rotor showed that the inlet guide vanes were overturning the air by approximately 4° across most of the annulus. In order to determine the performance of the compressor with the design entrance flow angles, the inlet guide vanes were reset to approximate more closely the design guide-vane turning. Several reports on airfoil cascades indicate that the change in turning angle is approximately 0.8 to 0.9 of the change in incidence angle. On this basis the inlet guide vanes were reset to a -5° incidence angle.

From a consideration of simple radial equilibrium after the guide vanes, the change in flow angle leaving the guide vanes will be accompanied by changes in the radial distribution of axial velocity and angle of attack at the entrance to the first rotor row. In order to determine the effects of this radial redistribution of the flow entering the compressor, the performance of the inlet stage and the over-all compressor performance were obtained for both the 0° and the -5° guide-vane incidence angles over a range of weight flow at speeds from 50 to 100 percent of design equivalent speed. A comparison of the results of the two phases of the investigation, which was conducted at the NACA Lewis laboratory, is presented herein.

APPARATUS AND INSTRUMENTATION

The 20-inch tip diameter, 10-stage axial-flow compressor reported in references 1 and 2 and schematically shown in figure 1 was used for the investigation. The test installation and instrumentation for the determination of the over-all compressor performance are the same as those presented in reference 1.

Moisture condensation, which resulted in corrosion of the flow passages and blading, took place after the use of refrigerated air during the initial investigation of the compressor. All rust was removed, and, in order to prevent further corrosion, the rotor, the stator casing, and all the blading were sprayed with a thin coat of heat-resistant aluminum paint before both phases of the present investigation. The painting of the flow passages reduced the peak efficiency of the compressor at all speeds, with the greatest decrease occurring at the low speeds. The compressor total-pressure ratio appeared to be unaffected by the change in surface finish.

The inlet stage comprised 36 circular-arc constant-thickness sheet-metal guide vanes, 25 rotor blades, and 27 stator blades. The design details are presented in reference 2. A sketch of the inlet guide vane, including some pertinent dimensions, is shown in figure 2.

Radial survey instrumentation, which was located at station 1 (after the inlet guide vanes) and at station 3 (after the first stator) as indicated in figure 1, consisted of a combination claw-total-pressure probe (fig. 3(a)) at each measuring station for the determination of the flow angle and the total pressure before and after the first stage. In addition, two five-tip spike-type radial thermocouple rakes (fig. 3(b)) were located at station 3. The thermocouples were calibrated over the range of Mach number encountered in this investigation. The instrument measuring stations were placed radially at area centers of equal annular areas before and after the inlet stage and around the periphery of the compressor so that they would be free of upstream instrument and blade wakes.

The inlet-stage total pressures were referenced to wall static-pressure taps at the same axial measuring station on U-tubes. The measuring fluid was tetrabromoethane. The temperature rise across the stage was measured on a potentiometer in conjunction with a spotlight galvanometer. Since the inlet stage operates stalled in the tip region of the annulus at low speeds, the accuracy of the measurements in this region is questionable. However, the consistency of the trends in the stall region appears to justify their use at least for comparison purposes.

PROCEDURE

The compressor was operated at equivalent speeds from 50 to 100 percent of design for both the 0° and -5° guide-vane incidence-angle investigations. At each speed a range of air flow was investigated from a maximum flow at which the compressor was choked to a minimum flow at which audible surge was encountered. The inlet pressure was varied to maintain a constant average Reynolds number of approximately 190,000 relative to the first rotor at the tip at all speeds. The over-all compressor performance was evaluated from a calculated discharge total pressure obtained from the average discharge static pressure, the total temperature, and the orifice weight flow with the method recommended in reference 3.

The stage temperature rise was measured differentially with the depression tank (station 0), and the total temperature was assumed to remain constant from the depression tank to station 1. The total pressures and total temperatures measured at station 3 were arithmetically

averaged for the five radial survey stations. With these averages and with the compressor-inlet conditions at station 1 and the air tables of reference 4, the total-pressure ratio and adiabatic temperature-rise efficiency of the inlet stage were determined. The inlet-stage performance is presented in terms of flow coefficient and equivalent total-pressure ratio, which method eliminates the speed parameter and results in a single performance curve that is essentially independent of speed. The stage performance parameters are derived in reference 5 and are also used in the following form in reference 6 (all symbols are defined in the appendix):

Flow coefficient:

$$\frac{Q}{UA_1} = \frac{WRT_1}{UA_1P_1}\left(1 + \frac{\gamma-1}{2}M_1^2\right)^{\frac{1}{\gamma-1}}$$

The Mach number was approximated from the ratio of the total pressure to the average wall static pressure at station 1.

Equivalent total-pressure ratio:

$$\left(\frac{P_3}{P_1}\right)_e = (Y_e + 1.0)^{\frac{\gamma}{\gamma-1}}$$

where

$$Y_e = K\frac{\Delta H_{is}}{U^2}$$

and

$$K = \left(\frac{U}{\sqrt{T_1}}\right)_d^2 \frac{1}{c_p}$$

RESULTS AND DISCUSSION

Compressor Performance

Guide-vane turning angle. - A comparison of the variation of guide-vane turning angle with radius ratio for both the 0° and -5° incidence-angle settings is presented in figure 4 at a high speed where the inlet stage is operating unstalled.

[redacted]

The guide vanes for the compressor were originally designed with the design rule for convergent annuli presented in reference 7. The fact that the guide vanes overturned the air as shown in figure 4 when set at 0° incidence angle may be attributed to the following factors:

(1) Corrections to the desired design guide-vane turning were applied to account for compressibility and hub taper. These corrections should not have been applied, because the design rule was determined from experimental data obtained in convergent annuli at inlet Mach numbers very close to those encountered in operating the compressor. The hub taper correction increased the guide-vane turning in this region by as much as 2°. The compressibility correction increased the turning from 0.2° at the hub to 0.7° at the tip.

(2) The accuracy of the design rule is approximately $\pm 1\frac{1}{4}^{\circ}$ over most of the vane height, which, if applied in the proper direction, may account for some of the guide-vane overturning.

(3) The manner in which the guide vanes were set with a straight edge between the leading and trailing edges of the vanes causes a deviation of approximately 0.5° to 1° from a chord-line setting. The magnitude of this deviation depends on the point along the blade span at which the vanes were set. Since the trailing-edge radius is smaller than the leading-edge radius of the vane, as shown in figure 2, the deviation in setting angle will also be in the direction of overturning the air.

Resetting the guide vanes to a -5° incidence angle in accordance with airfoil cascade data resulted in good agreement of the absolute flow angles with the design values (fig. 4).

Over-all performance characteristics. - A comparison of the compressor over-all performance characteristics with 0° and -5° guide-vane incidence angles is presented in figures 5(a) and (b) as total-pressure ratio and adiabatic temperature-rise efficiency plotted against equivalent weight flow over a range of equivalent speeds from 50 to 100 percent of design. The design-speed surge point was not obtained for the 0° guide-vane incidence angle; however, the curve in figure 5(a) was drawn to culminate at the surge line of the original over-all performance investigation (ref. 1). The design-speed surge point of reference 1 is represented by the large symbol (fig. 5(a)). At this point, the maximum total-pressure ratio increased from 7.52 to 7.66 for the -5° guide-vane incidence angle, with an attendant increase in equivalent weight flow from 53.7 to 54.6 pounds per second. The maximum weight flow at design speed increased approximately 2.6 percent, from 56.7 to 58.2 pounds per second.

The peak adiabatic temperature-rise efficiency (fig. 5(b)) increased approximately 1 point at design speed to 0.815 with the reduced

incidence angle. At low compressor speeds (50 to 70 percent of design), the effect of the guide-vane resetting appears to be negligible. The total-pressure ratio, adiabatic temperature-rise efficiency, and equivalent weight flow are the same within the accuracy of measurement at these speeds. These results indicate that design-speed performance was improved without seriously impairing the low-speed characteristics of the compressor by reducing the inlet guide-vane turning 5°. This fact can probably be attributed to the flat pressure-ratio characteristic of the inlet stage (ref. 6) when operating in the stall region at low speeds.

Surge-line characteristics. - As shown in figure 5(a) and as previously reported in reference 6, the compressor surge line had a slight knee at 70 percent of equivalent design speed. A comparison of the original surge line (0° guide-vane incidence angle) and that obtained with the reduced incidence angle is shown in figures 5(a) and (c). The knee in the compressor surge line is usually characterized by an abrupt increase in surge equivalent weight flow, total-pressure ratio, and adiabatic temperature-rise efficiency with increasing speed, as shown in figure 5(c), where these parameters are plotted against percentage of equivalent design speed for both investigations. The effect of the guide-vane resetting was to move the knee in the compressor surge line from 70 to 73 percent of equivalent design speed.

Static-pressure-ratio distributions. - The effect of guide-vane resetting on the over-all, stage, and blade-row static-pressure ratios obtained from the outer wall static taps is shown in figure 6. The comparison is made at an over-all compressor static-pressure ratio of approximately 6.25, which corresponds to the peak-efficiency point at design speed for both guide-vane settings, in order to determine how the stage loading varied through the compressor in obtaining the same over-all pressure ratio. The figure indicates that only the first-stage rotor is seriously affected by the change in guide-vane incidence angle. The increased static-pressure rise across the first rotor must be compensated for by a smaller rise in some other stage or stages. It is evident from figure 6 that the smaller rise in static-pressure ratio is spread out among the remaining blade rows so that the effect appears negligible. Consequently, the increase in pressure ratio obtained at a given flow condition can probably be attributed primarily to the increased loading on the first rotor row.

Inlet-Stage Performance

The discussion of the over-all compressor performance presented in the previous sections indicates that the inlet stage is primarily responsible for the changes in over-all compressor performance obtained when the guide-vane incidence angle is reduced. In the following sections, the effect of the guide-vane resetting on the inlet-stage performance

and its subsequent effect on the over-all performance are analyzed on the basis of the radial distribution of flow conditions entering the first rotor and the blade-element performance at five radii across the inlet stage.

Inlet-stage over-all performance characteristics. - The over-all performance characteristics of the inlet stage are presented as dimensionless parameters of equivalent total-pressure ratio and adiabatic temperature-rise efficiency against flow coefficient in figure 7. The data are incomplete at design speed because of moisture condensation and subsequent freezing on the probes and in the manometer lines when testing with refrigerated air. The peak equivalent total-pressure ratio of the inlet stage increased from a value of approximately 1.200 to 1.225 with the decreased incidence angle on the inlet guide vanes. The peak of the curve also occurred at a higher flow coefficient for the decreased incidence. This latter effect might be expected, since the flow coefficient can be reduced to a ratio of axial velocity to wheel speed. For any given absolute flow angle entering a rotor row, the relative flow angle (and, hence, the angle of attack) is a function of the ratio of axial velocity to wheel speed and hence flow coefficient. Decreasing the guide-vane incidence angle, which increases the angle of attack on the first rotor, will cause the angle of attack for peak pressure ratio to occur at a higher equivalent weight flow. The increase in flow coefficient required to obtain the same average angle of attack on the first stage for the reduced guide-vane incidence will displace the performance curve shown in figure 7 toward a higher flow coefficient. The increase in peak equivalent total-pressure ratio of the inlet stage can be partially attributed to the higher flow coefficient at which the peak value is obtained. At the higher flow coefficient, the increase in axial velocity required to obtain the same average angle of attack while maintaining the same turning angle through the rotor will increase the change in tangential velocity across the rotor and thereby increase the total-pressure ratio of the stage. The difference in peak efficiency at the two guide-vane incidence angles for the inlet stage is believed to be within the accuracy of the measurements obtained.

Flow conditions at entrance to first rotor row. - The investigation of the inlet stage with the 0° guide-vane incidence also included radial surveys of static pressure at station 1, which permitted the direct calculation of the flow velocities entering the first rotor. The flow velocities and angles of attack entering the first rotor were also calculated with the measured flow angles leaving the guide vanes and simple radial equilibrium with the following equation from reference 8 (in the nomenclature of this report):

[redacted]

$$\frac{V_a}{V_{a,ref}} = \frac{\cos \beta_1}{\cos \beta_{1,ref}} e^{-\int_{z_{1,ref}}^{z_1} \frac{\sin^2 \beta_1}{z_1} dz}$$

where

$$V_{ref} = \frac{V_{a,ref}}{\cos \beta_{1,ref}}$$

3003

The reference velocity after the guide vanes was determined near the tip from the wall static pressure and the corresponding total pressure obtained at the radial measuring station closest to the casing, except for the calculation at low speeds, where the reference velocity was adjusted to more nearly satisfy continuity. A comparison of the measured and calculated angles of attack at the 0° guide-vane incidence is presented for three flow coefficients in figure 8(a). The agreement with simple radial equilibrium at all flow coefficients is fairly good. The agreement between measured and calculated values at 0° guide-vane incidence justified the use of the simple-radial-equilibrium method in determining the flow velocities and angles of attack entering the first rotor for both guide-vane incidence settings. Since no static-pressure surveys were obtained for the -5° guide-vane incidence, the simple-radial-equilibrium calculation method of determining the flow velocities was used to obtain a common basis of comparison for the two guide-vane settings.

The radial distribution of axial-velocity ratio and of angle of attack for both guide-vane incidence angles is presented for three flow coefficients in figures 8(b) and (c), respectively. In order to satisfy the simple-radial-equilibrium relation, the decrease in guide-vane discharge angle shown in figure 4 requires an increase in axial velocity at the tip and a decrease at the hub (fig. 8(b)). At the same flow coefficient, the average angle of attack for the reduced guide-vane incidence will be increased; however, the change in axial-velocity distribution required to satisfy simple radial equilibrium produces a smaller increase in angle of attack at the tip than at the hub (fig. 8(c)). In order to determine the effects on the inlet-stage performance of this radial redistribution of flow conditions entering the first rotor row, a study of the blade-element data is necessary.

Stage-element performance. - The performance of the inlet stage at five radial elements from tip to hub is presented in figure 9 as equivalent total-pressure ratio and adiabatic temperature-rise efficiency

plotted against angle of attack. The angle of attack was computed from the guide-vane turning and simple radial equilibrium, as described in the previous section. The equivalent total-pressure ratio obtained at all five radial positions is higher for the same angle of attack for the -5° than for the 0° guide-vane incidence angle at the higher speeds where the inlet stage is operating unstalled. The efficiency of each stage element remained approximately the same. The angle-of-attack range of the blade section near the tip (radial position a, fig. 9(a)) for any given speed moves to a slightly higher set of values of angle of attack for the reset guide vanes. However, at design speed the angle of attack at the choke-flow point is approximately 1.5° for both guide-vane incidence-angles. Therefore, the weight-flow limitation of this compressor at high speeds appears to be caused by choking of the tip sections of the inlet stage. This effect was indicated in the inter-stage performance investigation reported in reference 6.

At low compressor speeds, where the tip section is severely stalled, the effect of increasing the angle of attack is negligible. The efficiency of this section (fig. 9(a)) drops rapidly at angles of attack higher than approximately 19°, which indicates a stage-element stall at this point. As could be expected, the stall angle of attack is unaffected by the change in guide-vane incidence angle.

At each successive radial element toward the hub (figs. 9(b) to (e)) the angle-of-attack range moves toward an increasingly higher value, as was previously indicated by the change in radial distribution of angle of attack in figure 8(c). At radial positions b and c (figs. 9(b) and (c)), the stage-element stall occurs at an angle of attack of approximately 23° and 26°, respectively. The stage elements closest to the hub (d and e, figs. 9(d) and (e)) do not appear to have a definite stall point, as indicated by the elimination of the sharp drop in efficiency that usually accompanies stall.

The higher equivalent total-pressure ratio obtained across the inlet stage with the reset guide vanes could be attributed to the higher flow coefficient at which the same average angle of attack was obtained. From a consideration of the radial redistribution of angle of attack entering the first rotor for the reduced guide-vane incidence, the hub elements would do more work when the stage is operating at the same average angle of attack than the tip elements. The stage-element data, however, indicate that all the elements of the inlet stage are operating with approximately the same increase in equivalent total-pressure ratio. The uniform increase in total-pressure ratio obtained radially, rather than the expected larger increase at the hub than at the tip, can be explained from a study of typical velocity vector diagrams in conjunction with the results of reference 9. The radial distribution of flow conditions entering the first rotor for the case in which the mean-radius

angle of attack is the same for both guide-vane settings is shown in figure 10. The vector diagrams are presented in terms of velocity ratios for the tip, mean, and hub radial positions in figure 11.

The variation of turning angle with angle of attack was determined from the cascade data of reference 10. The stage pressure rise is a direct function of the change in tangential velocity across the rotor. As can be seen on the velocity diagrams of figure 11, the change in tangential velocity is dependent on the turning angle, the relative inlet velocity, and the change in axial velocity across the rotor. At the tip radial position, the decreased angle of attack shown in figures 10 and 11(a) for the reduced guide-vane incidence will tend to decrease the total-pressure ratio, while the increased relative inlet velocity shown in figure 10 and the greater reduction in axial velocity across the rotor tip indicated by reference 9 will tend to increase the total-pressure ratio. Thus, if the latter two effects dominate as shown on figure 11(a), a greater total-pressure rise would be obtained than would be expected from the increase in flow coefficient alone.

At the mean-radius position (fig. 11(b)), where the angle of attack was selected to be identical for both guide-vane incidence angles, the greater total-pressure rise can be attributed primarily to the increased relative inlet velocity. Reference 9 indicates that the change in axial velocity across the rotor will remain about the same at the mean-radius blade section for both guide-vane settings.

Near the hub, the angle of attack and relative inlet velocity will be greater for the reduced guide-vane incidence (figs. 10 and 11(c)) and will increase the pressure ratio, while the axial-velocity ratio will increase across the rotor hub (ref. 9) and tend to decrease the pressure ratio. The relative discharge flow angle from the rotor is sufficiently small near the hub that the change in axial velocity has little effect on the change in tangential velocity.

Effect of Guide-Vane Resetting on Compressor Performance

In order to point out some of the complications that may arise because of guide-vane resetting and to indicate the direction of the effects on the performance characteristics of axial-flow compressors, a simple-radial-equilibrium analysis of the flow conditions entering the first rotor row of this compressor was made for guide-vane incidence angles of 20° to -10°. This analysis required a knowledge of the absolute flow angles leaving the guide vanes. Therefore, it was assumed that the change in guide-vane turning angle would be 0.8 of the change in incidence angle at all radii. The change in guide-vane turning was then applied to the average measured guide-vane angles obtained in the high flow-coefficient range at 0° guide-vane incidence to obtain the new guide-vane turning angles for the selected incidence angle. The

radial distribution of axial velocity required to satisfy simple radial equilibrium is shown in figure 12(a) as the ratio of axial velocity to the mean-radius axial velocity for guide-vane incidence angles from 20° to -10°. The change in axial-velocity distribution will cause much smaller changes in angle of attack in the tip region than near the hub, as shown in figures 12(b) and (c), where the radial distribution of angle of attack at a high and at a low flow coefficient is presented over a range of guide-vane incidence angles from 20° to -10°. At the higher flow coefficient, the change in angle of attack for a given change in guide-vane incidence is much greater than at the lower flow coefficient. The magnitude of the angles of attack at the low flow coefficient indicates that the tip blade sections will probably operate in the stall region within the practical range of guide-vane adjustment.

Adjustable guide vanes have been used in some jet engines in an attempt to alleviate starting and acceleration problems. Improvement in starting and accelerating characteristics could be obtained by increasing the low-speed efficiency of the compressor by adjusting the inlet guide vanes toward highly positive incidence angles and thus allowing the first-stage rotor to operate closer to design angle of attack. The reduction in angle of attack on the inlet stage is caused by the twofold effects of the increase in guide-vane incidence combined with the increase in weight flow obtained because of unchoking of the exit stages at low speeds. The improvement in angle of attack will occur primarily in the hub blade section, as indicated in figures 12(b) and (c). Since these blade sections normally operate efficiently over a very wide range of angle of attack (figs. 9(d) and (e)), little improvement in inlet-stage efficiency could be obtained. The radial rematching in the first rotor and the stage interaction effects downstream of the first rotor would determine the over-all compressor efficiency.

The knee that occurs in the surge line of most high-pressure-ratio compressors has prevented some engines from accelerating to design speed. The point at which the knee occurs has been associated with stall of the inlet stage, as indicated in references 5 and 6; and the magnitude of the knee appears to be affected by the stage interaction effects that occur downstream of the stalled stage. Increasing the guide-vane incidence will cause the knee in the compressor surge line to occur at a lower speed and weight flow (ref. 5); while decreasing the guide-vane incidence will shift the knee to a higher speed and flow (fig. 5(a)). The magnitude of the knee will increase when it occurs at a higher speed because of the higher pressure level at which the inlet stages are operating. At speeds below the knee in the surge line, increasing the guide-vane incidence will tend to increase weight flow through the compressor, because the higher pressure ratio of the inlet stage will unchoke the exit stages. At speeds above the knee in the surge line, the increased guide-vane incidence would decrease the flow, because the inlet stage would operate at lower angles of attack, and, thus, the pressure ratio would be reduced and the exit stages would choke at a lower flow.

[redacted]

The knee in the compressor surge line may not be eliminated by guide-vane adjustment, but the location of the knee may be changed within limits, as evidenced by the results of this experimental investigation and those of reference 5. The analysis and experimental data indicate that large guide-vane adjustments would be required in order to improve the starting and acceleration characteristics of a jet engine.

Slight guide-vane adjustments can be used effectively in improving the design-speed performance of a given compressor. Efficiency assumptions and boundary-layer allowances used in the design of a compressor determine the area ratios and the design weight flow. Since these assumptions are based on fragmentary experimental results and are subject to errors, design-point operation is usually not obtained. In order to compensate for these errors and to obtain approximately design angles of attack on all stages in the compressor, slight guide-vane adjustments can be made that will increase or decrease the weight flow at design over-all total-pressure ratio as needed. These small changes in guide-vane incidence will probably have very little effect on the low- and intermediate-speed performance of the compressor.

3003

SUMMARY OF RESULTS AND CONCLUSIONS

The inlet-guide-vane incidence angle of a 10-stage subsonic axial-flow compressor was reduced 5° in order to approximate more closely the design flow conditions entering the first rotor. The effects of the reduced guide-vane incidence on the over-all and inlet-stage performance of the compressor were as follows:

1. With the reduced guide-vane incidence, the surge pressure ratio increased from 7.52 to 7.66, the maximum equivalent weight flow increased from 56.7 to 58.2 pounds per second, and the peak efficiency increased approximately 1 point to 0.815 at design speed.

2. At speeds below the knee in the surge line, reducing the guide-vane incidence 5° had a negligible effect on the compressor performance. At speeds above the knee in the surge line, the choke weight flow and surge pressure ratio were increased.

3. The compressor surge line remained unchanged except in the intermediate-speed range. The initiation of the knee in the surge line increased from 70 to 73 percent of equivalent design speed, and the magnitude of the knee was slightly greater at the reduced guide-vane incidence.

4. The wall static-pressure ratios through the compressor indicated that only the performance of the first rotor row was affected by the guide-vane resetting, with no appreciable change in the loading distribution of the remaining blade rows.

5. The peak equivalent total-pressure ratio of the inlet stage was increased from 1.200 to 1.225 with approximately the same efficiency. The peak efficiency and peak equivalent total pressure occurred at a higher flow coefficient at the reduced guide-vane incidence. The equivalent total-pressure ratio obtained across each of five radial elements of the inlet stage was greater at the same angle of attack on a given element for the -5° guide-vane setting.

6. Analysis and experimental data indicate that very large guide-vane adjustments would be required in order to improve the starting and acceleration characteristics of a jet engine.

7. Small changes in inlet-guide-vane setting appear to be a feasible means of correcting for efficiency and boundary-layer assumptions used in a compressor design so that design-point operation may be obtained.

Lewis Flight Propulsion Laboratory
National Advisory Committee for Aeronautics
Cleveland, Ohio, August 24, 1953

[redacted]

APPENDIX - SYMBOLS

The following symbols are used in this report:

A	annulus area, sq ft
c	blade chord, in.
c_p	specific heat at constant pressure, Btu/(lb)($^{\circ}$F)
H	total enthalpy, Btu/lb
i	angle of incidence, angle between tangent to blade camber line at leading edge and inlet-air direction, deg
M	Mach number
P	total pressure, in. Hg abs
p	static pressure, in. Hg abs
Q	volume flow, cu ft/sec
R	gas constant, ft-lb/(lb)($^{\circ}$F)
T	total temperature, $^{\circ}$R
U	rotor tip speed, ft/sec
V	absolute velocity, ft/sec
W	weight flow, lb/sec
Y	pressure-ratio function, $\left(\frac{P_n}{P_{n-2}}\right)^{\frac{\gamma-1}{\gamma}} - 1$
z	radius ratio
α	angle of attack, deg
β	absolute inlet air angle, angle between compressor axis and absolute air velocity, deg
γ	ratio of specific heats
δ	ratio of total pressure to standard sea-level pressure
η	adiabatic temperature-rise efficiency

3003

[redacted]

θ	ratio of total temperature to standard sea-level temperature
μ	blade camber angle, deg
σ	solidity, ratio of chord to spacing
φ	blade setting angle, angle between compressor axis and blade chord

3003

Subscripts:

a	axial
d	design conditions
e	equivalent, indicates that the parameter to which it is affixed has been corrected to design speed
is	isentropic process
m	mean radius
n	station number
ref	reference
0	inlet depression tank
1	discharge of inlet guide vane
2,4,6 . . . 20	stations behind rotors, first, second, third, . . . tenth stage
3,5,7 . . . 21	stations behind stators, first, second, third, . . . tenth stage
22	discharge of exit guide vanes

Superscript:

'	relative to rotor blade row

REFERENCES

1. Budinger, Ray E., and Thomson, Arthur R.: Investigation of a 10-Stage Subsonic Axial-Flow Research Compressor. II - Preliminary Analysis of Over-All Performance. NACA RM E52C04, 1952.

2. Johnsen, Irving A.: Investigation of a 10-Stage Subsonic Axial-Flow Research Compressor. I - Aerodynamic Design. NACA RM E52B18, 1952.

3. NACA Subcommittee on Compressors: Standard Procedures for Rating and Testing Multistage Axial-Flow Compressors. NACA TN 1138, 1946.

4. Keenan, Joseph H., and Kaye, Joseph: Thermodynamic Properties of Air. John Wiley & Sons, Inc., 1947.

5. Medeiros, Arthur A., Benser, William A., and Hatch, James E.: Analysis of Off-Design Performance of a 16-Stage Axial-Flow Compressor with Various Blade Modifications. NACA RM E52L03, 1953.

6. Budinger, Ray E., and Serovy, George K.: Investigation of a 10-Stage Subsonic Axial-Flow Research Compressor. IV - Individual Stage Performance Characteristics. NACA RM E53C11, 1953.

7. Lieblein, Seymour: Turning-Angle Design Rules for Constant-Thickness Circular-Arc Inlet Guide Vanes in Axial Annular Flow. NACA TN 2179, 1950.

8. Finger, Harold B.: Method of Experimentally Determining Radial Distributions of Velocity through Axial-Flow Compressor. NACA TN 2059, 1950.

9. Jackson, Robert J.: Effects on the Weight-Flow Range and Efficiency of a Typical Axial-Flow Compressor Inlet Stage that Result from the Use of a Decreased Blade Camber or Decreased Guide-Vane Turning. NACA RM E52G02, 1952.

10. Herrig, L. Joseph, Emery, James C., and Erwin, John R.: Systematic Two-Dimensional Cascade Tests of NACA 65-Series Compressor Blades at Low Speeds. NACA RM L51G31, 1951.

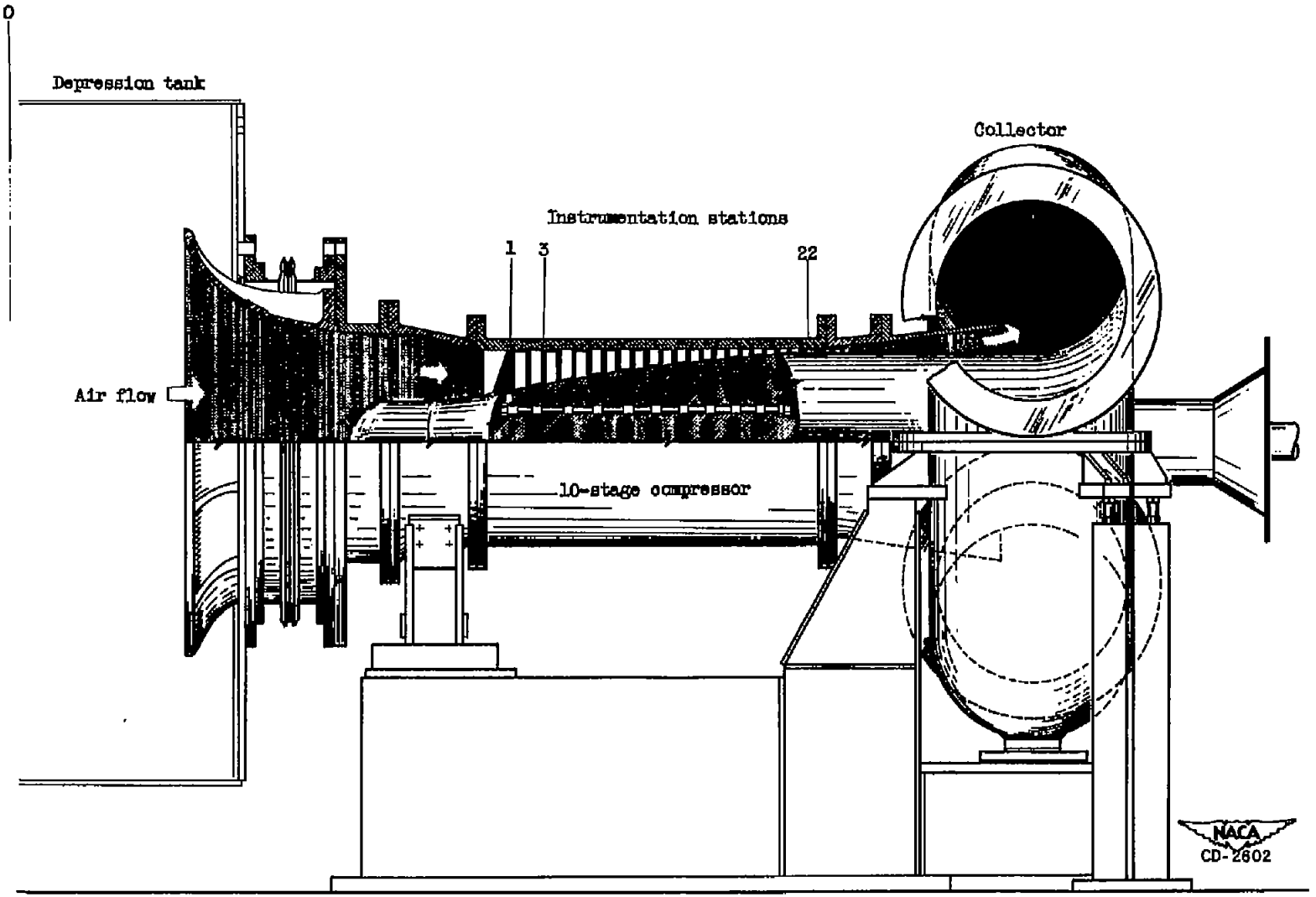

Figure 1. - Cross-sectional view of 10-stage compressor showing instrumentation stations.

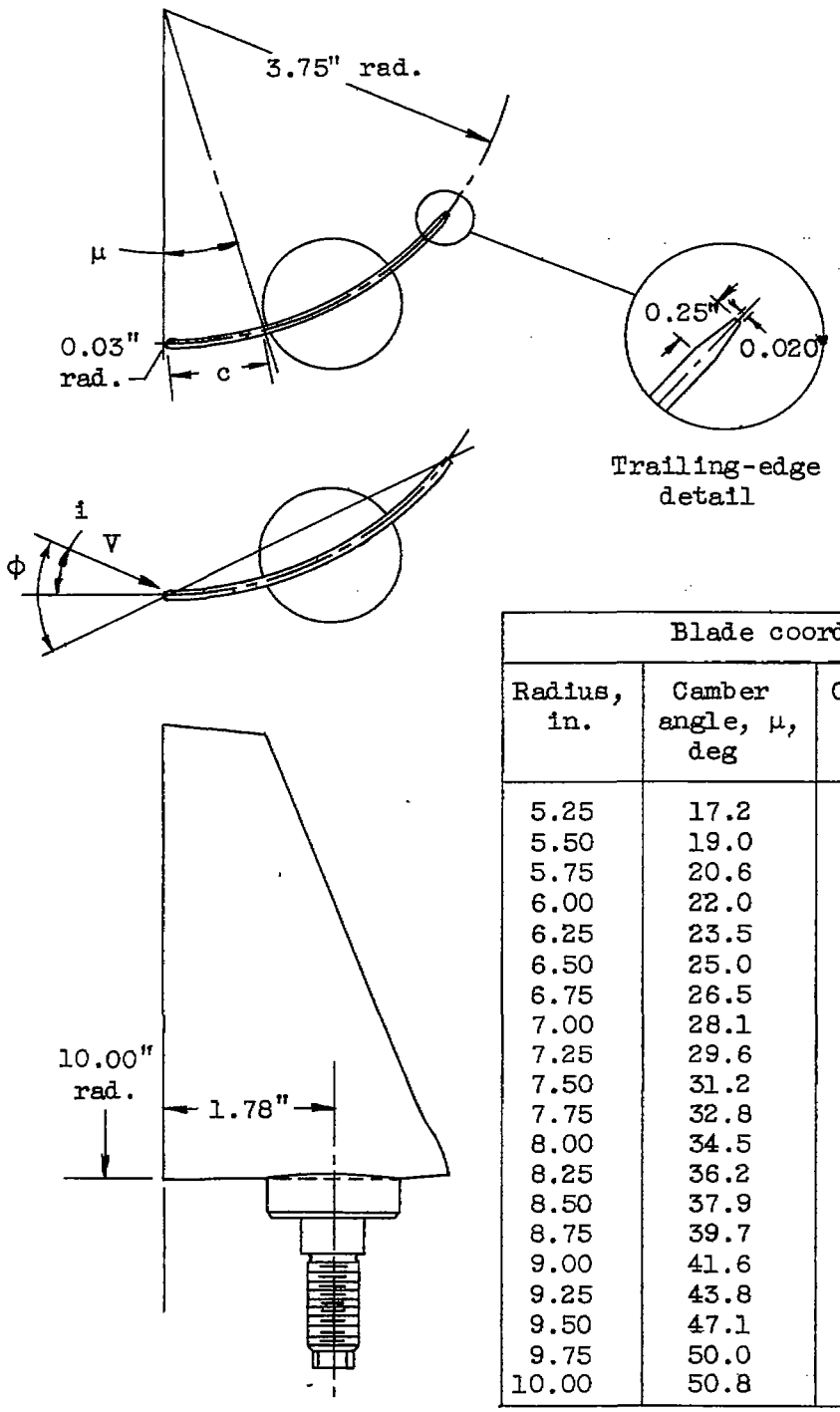

Blade coordinates			
Radius, in.	Camber angle, μ, deg	Chord, c, in.	Solidity, σ
5.25	17.2	1.134	1.238
5.50	19.0	1.238	-----
5.75	20.6	1.341	-----
6.00	22.0	1.431	1.367
6.25	23.5	1.527	-----
6.50	25.0	1.623	-----
6.75	26.5	1.719	-----
7.00	28.1	1.821	1.491
7.25	29.6	1.916	-----
7.50	31.2	2.017	-----
7.75	32.8	2.118	-----
8.00	34.5	2.224	1.593
8.25	36.2	2.330	-----
8.50	37.9	2.436	-----
8.75	39.7	2.547	-----
9.00	41.6	2.663	1.695
9.25	43.8	2.797	-----
9.50	47.1	2.997	-----
9.75	50.0	3.168	-----
10.00	50.8	3.217	1.843

Figure 2. - Inlet guide vane. Number 14-gage (0.083) mild steel.

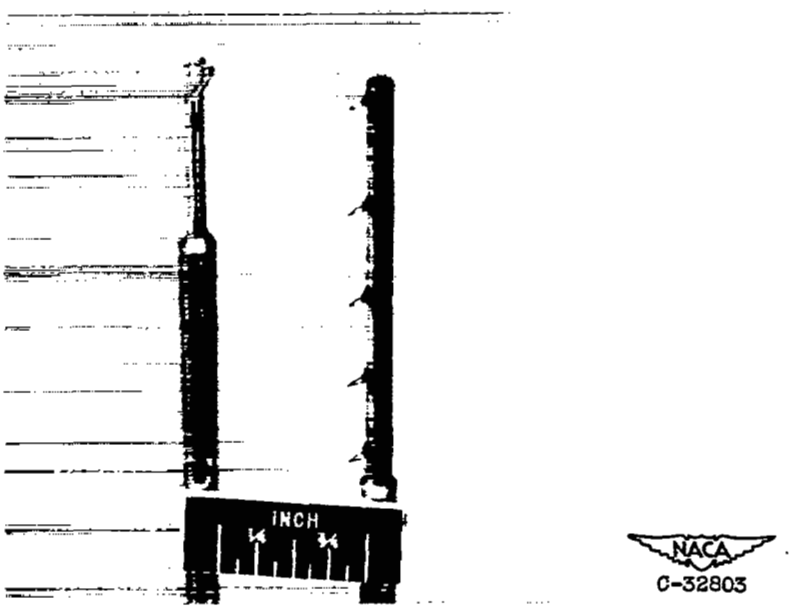

(a) Combination claw total-pressure survey probe.

(b) Spike-type radial thermocouple rake.

Figure 3. - Inlet-stage instrumentation.

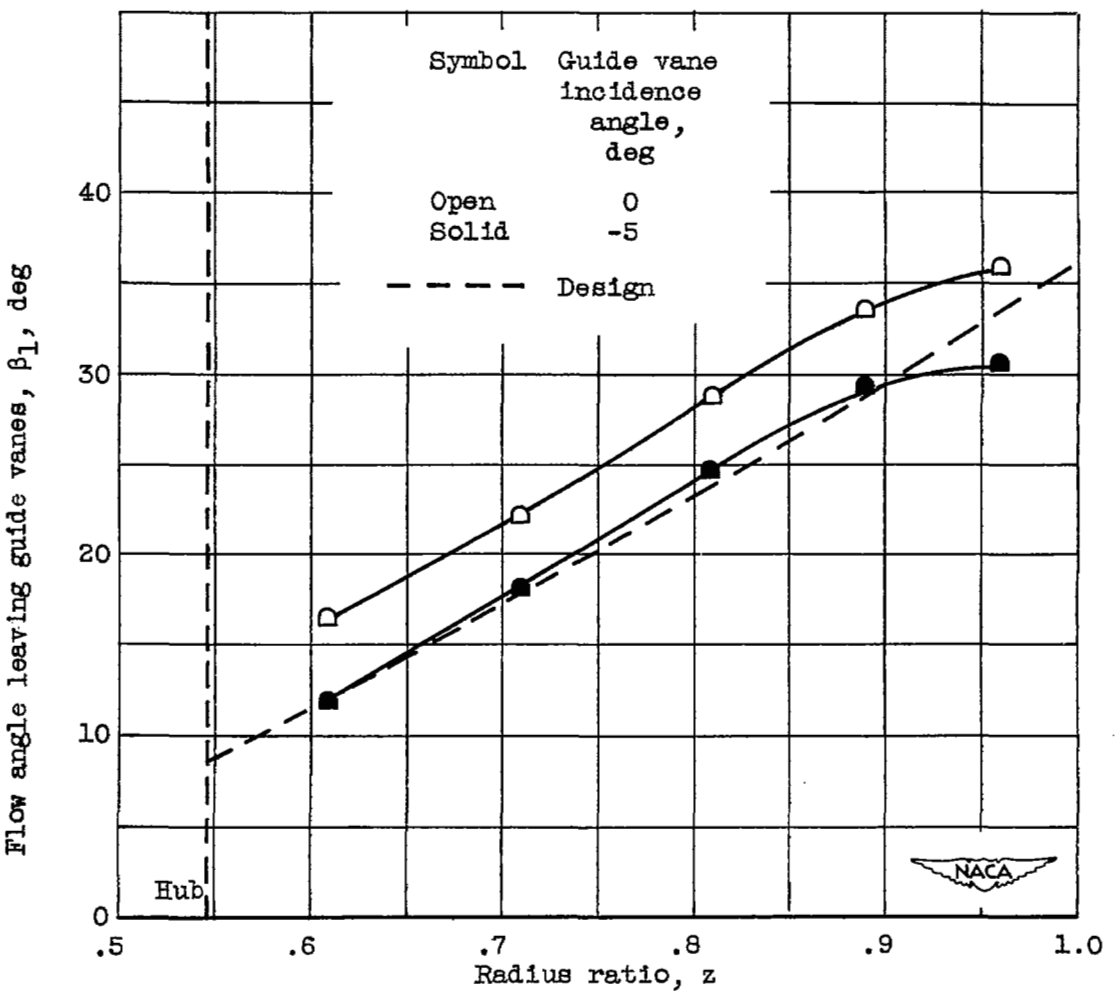

Figure 4. - Comparison of radial distribution of flow angle leaving guide vanes for 0° and -5° guide-vane incidence angles. Speed, 90-percent design; flow coefficient, 0.615.

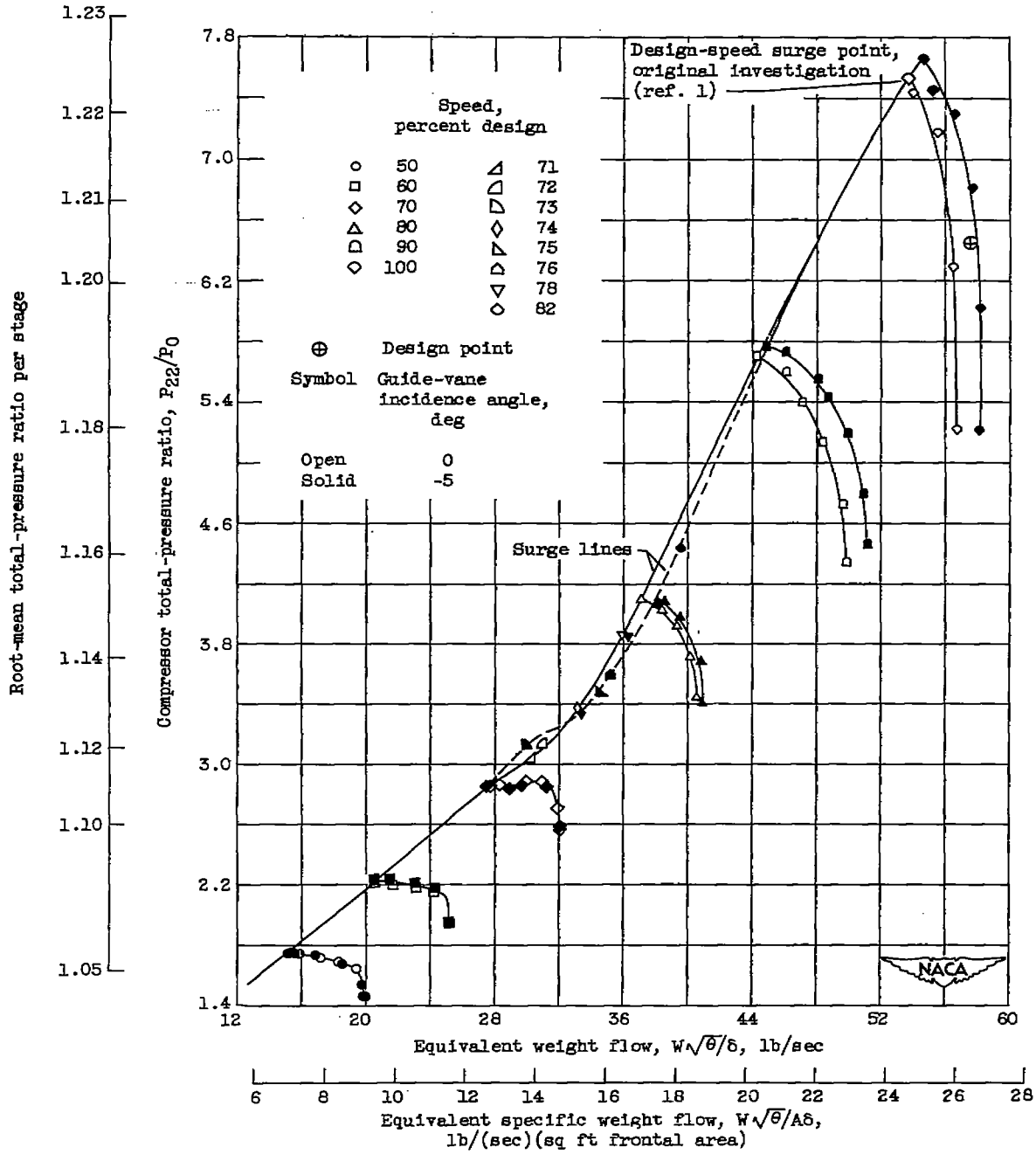

(a) Compressor total-pressure ratio and root-mean total-pressure ratio per stage.

Figure 5. - Over-all performance of 10-stage subsonic axial-flow compressor at guide-vane incidence angles of 0° and -5° over range of weight flow at speeds from 50 to 100 percent of equivalent design speed.

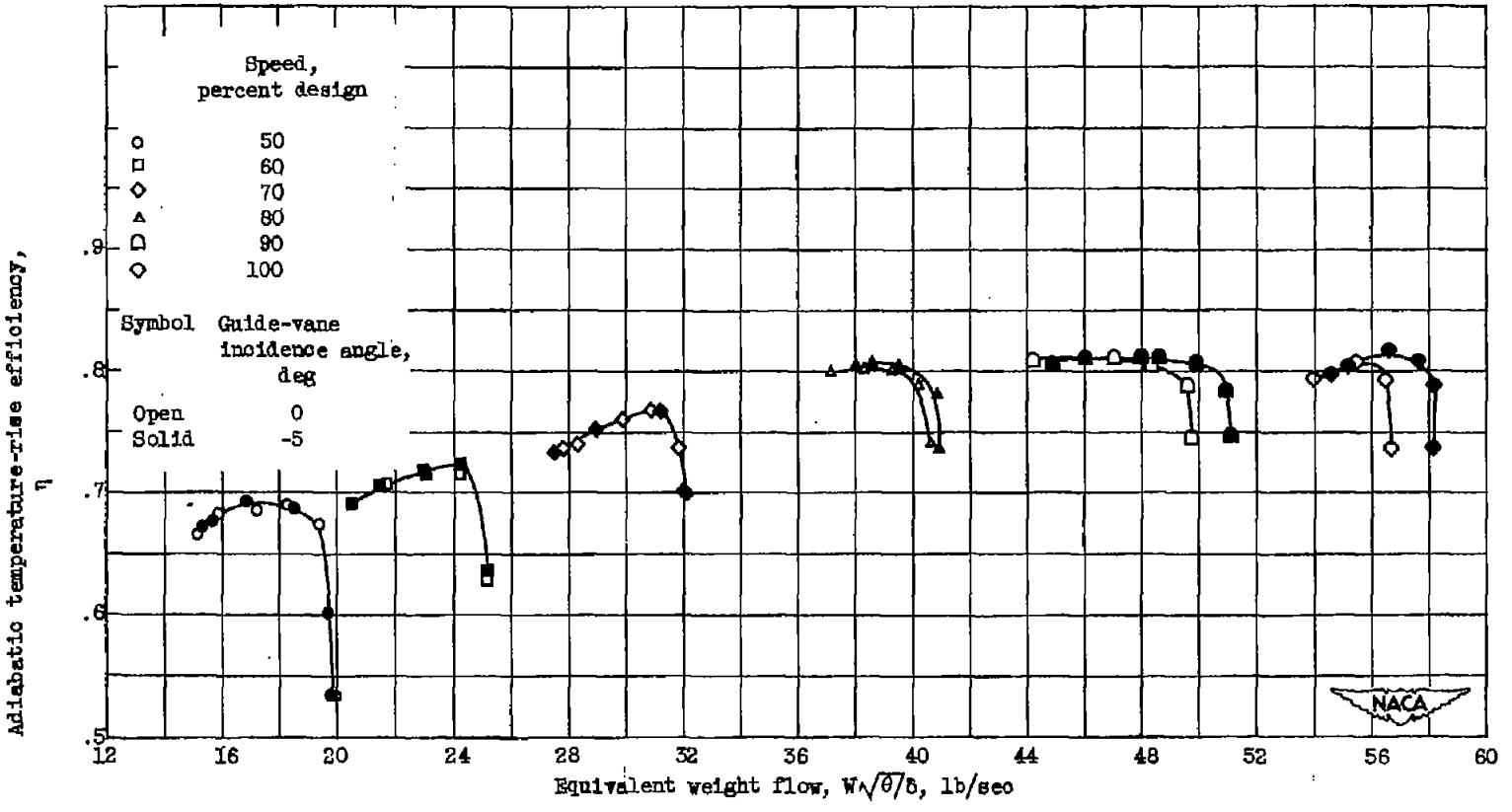

(b) Adiabatic temperature-rise efficiency.

Figure 5. - Continued. Over-all performance of 10-stage subsonic axial-flow compressor at guide-vane incidence angles of 0° and -5° over range of weight flow at speeds from 50 to 100 percent of equivalent design speed.

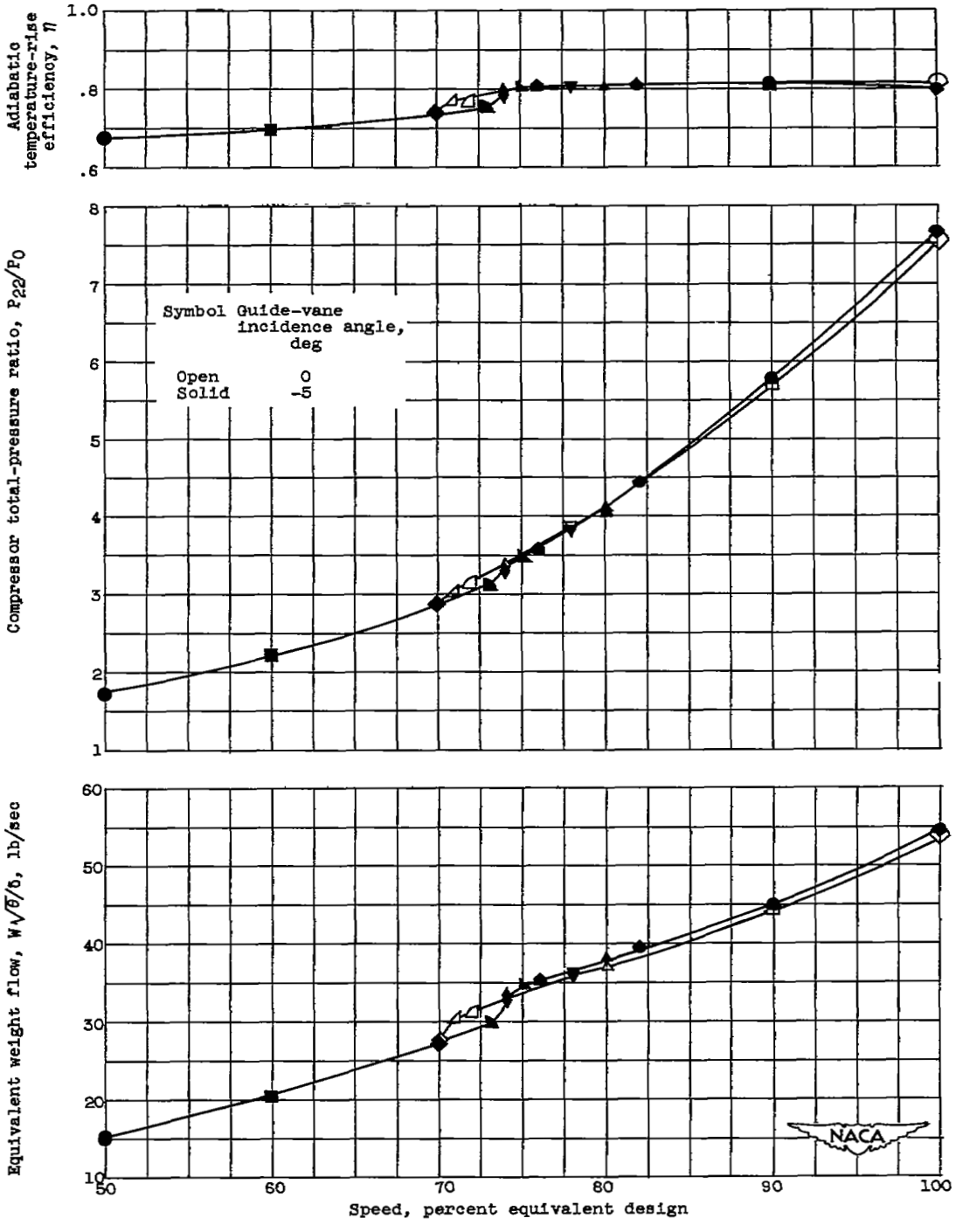

(c) Adiabatic temperature-rise efficiency, compressor total-pressure ratio, and equivalent weight flow at surge against percent of equivalent design speed.

Figure 5. - Concluded. Over-all performance of 10-stage subsonic axial-flow compressor at guide-vane incidence angles of 0° and -5° over range of weight flow at speeds from 50 to 100 percent of equivalent design speed.

[redacted]

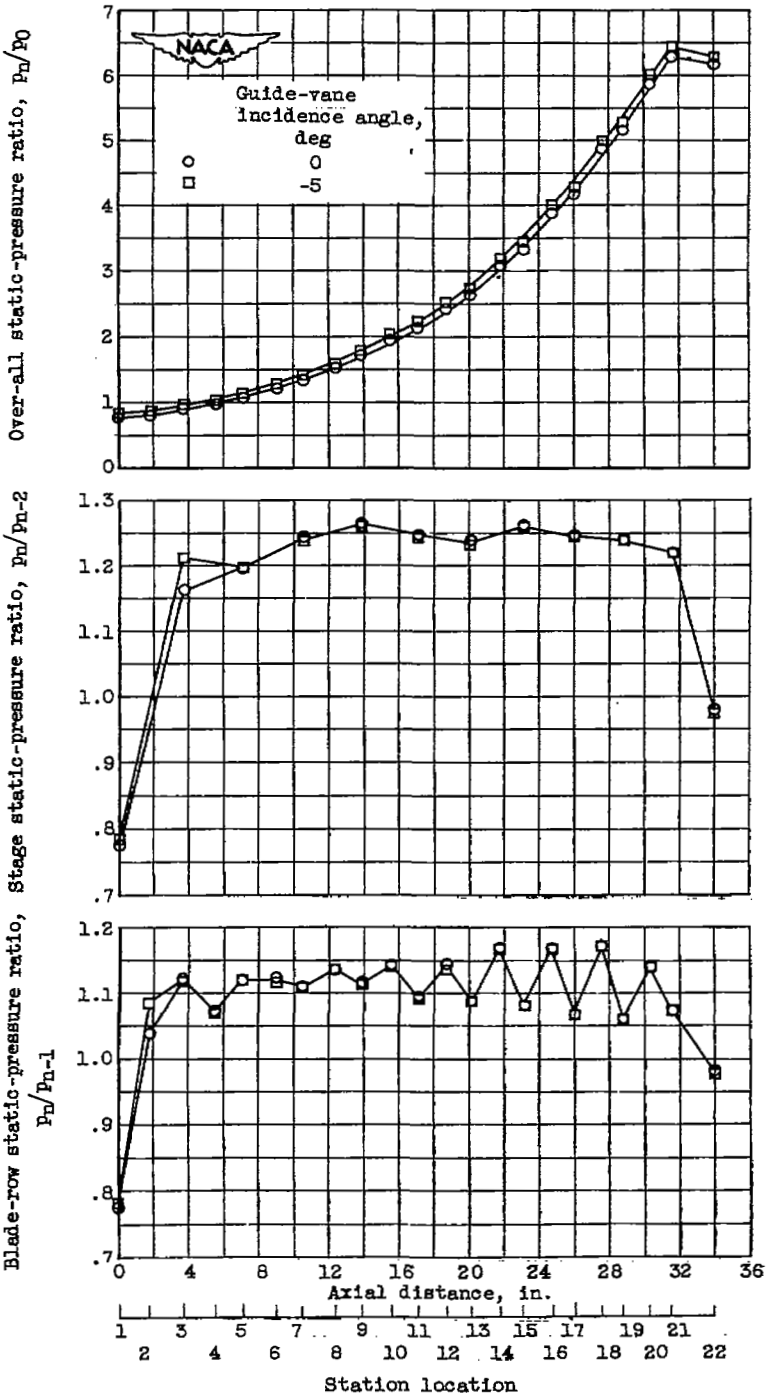

Figure 6. - Static-pressure-ratio distributions for 0° and -5° guide-vane incidence at over-all static-pressure ratio of approximately 6.25 at design speed.

[redacted]

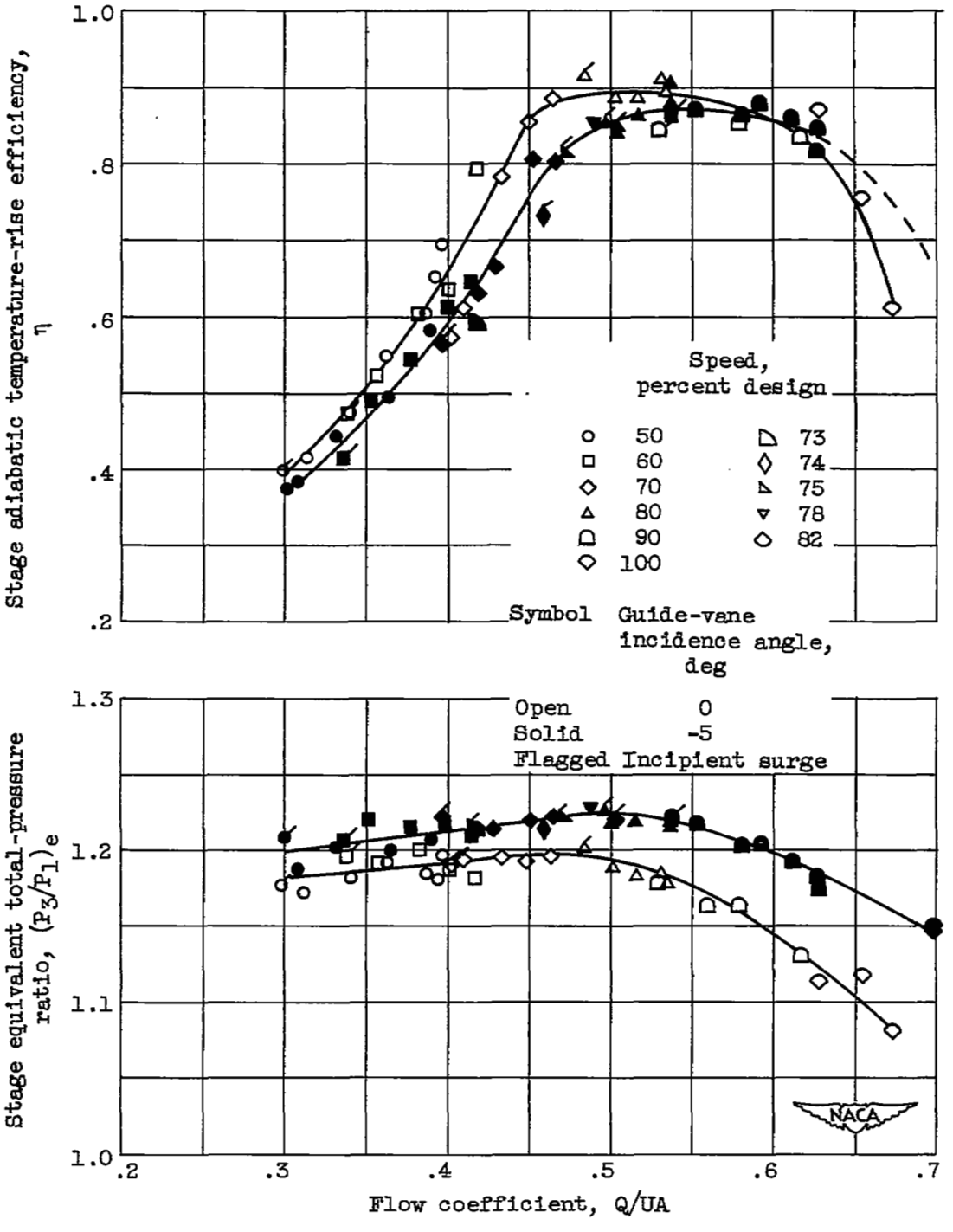

Figure 7. - Comparison of inlet-stage performance for 0° and -5° guide-vane incidence angles over range of weight flow at speeds from 50 to 100 percent of equivalent design speed.

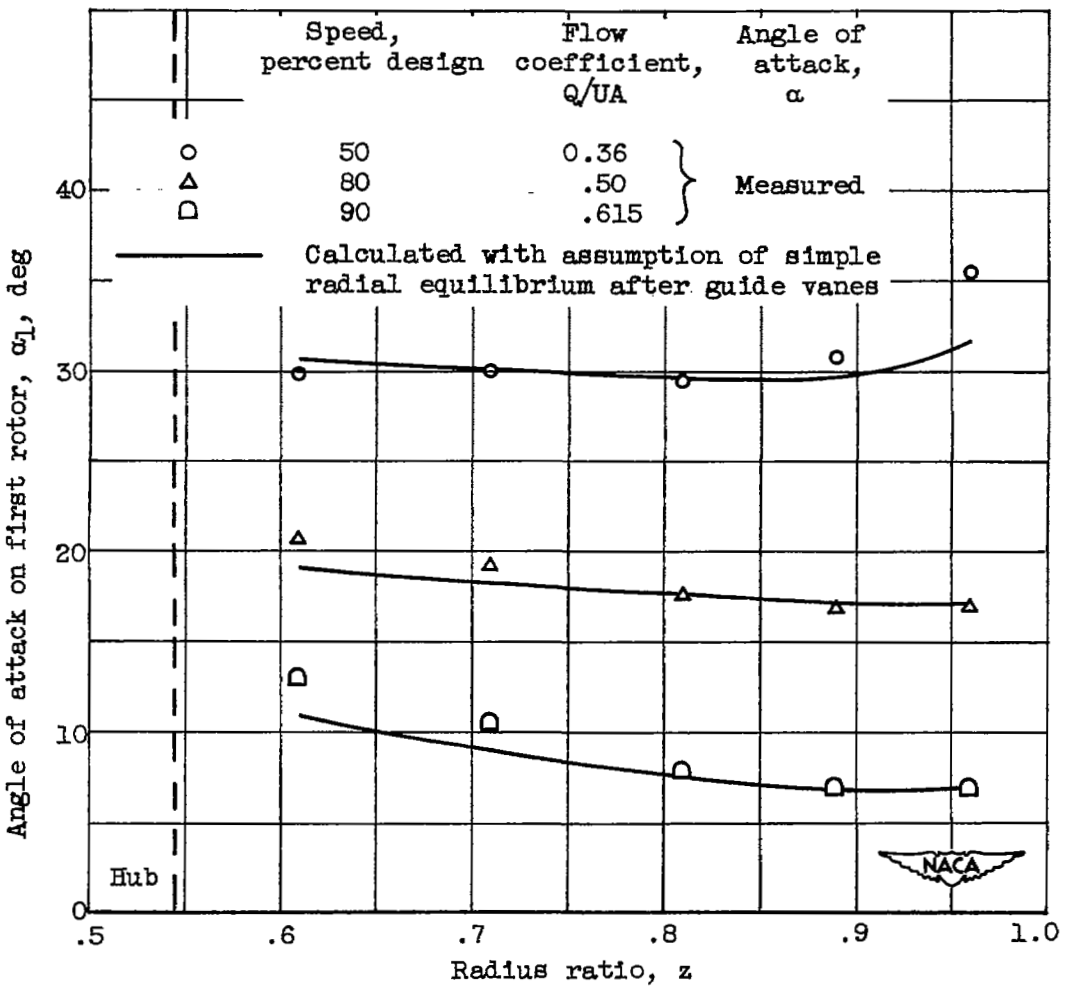

(a) Measured and calculated angles of attack. Guide-vane incidence angle, 0°

Figure 8. - Angle of attack and axial velocity on first rotor at three flow coefficients.

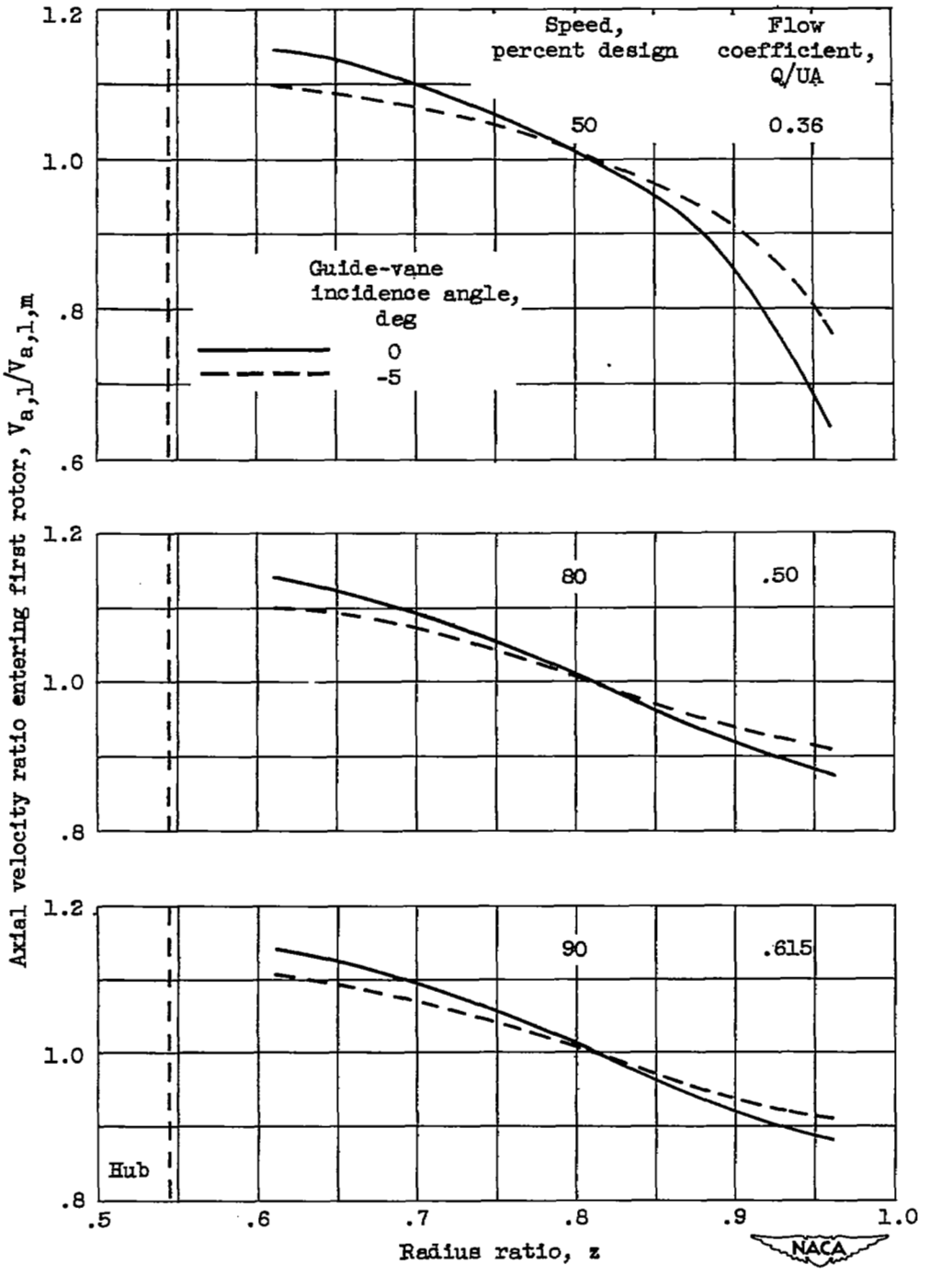

(b) Axial-velocity distribution.

Figure 8. - Continued. Angle of attack and axial velocity on first rotor at three flow coefficients.

[redacted]

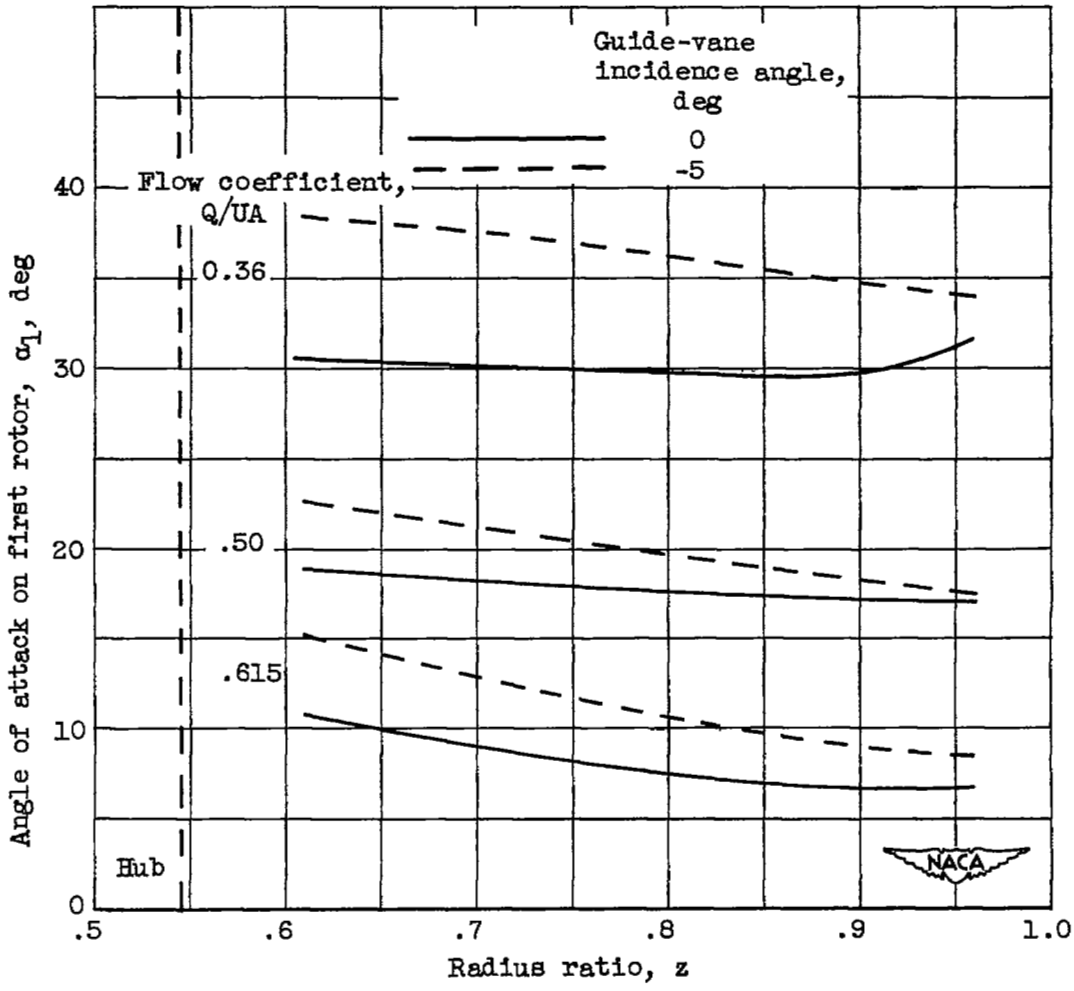

(c) Angle of attack calculated with assumption of simple radial equilibrium after guide vanes.

Figure 8. - Concluded. Angle of attack and axial velocity on first rotor at three flow coefficients.

[redacted]

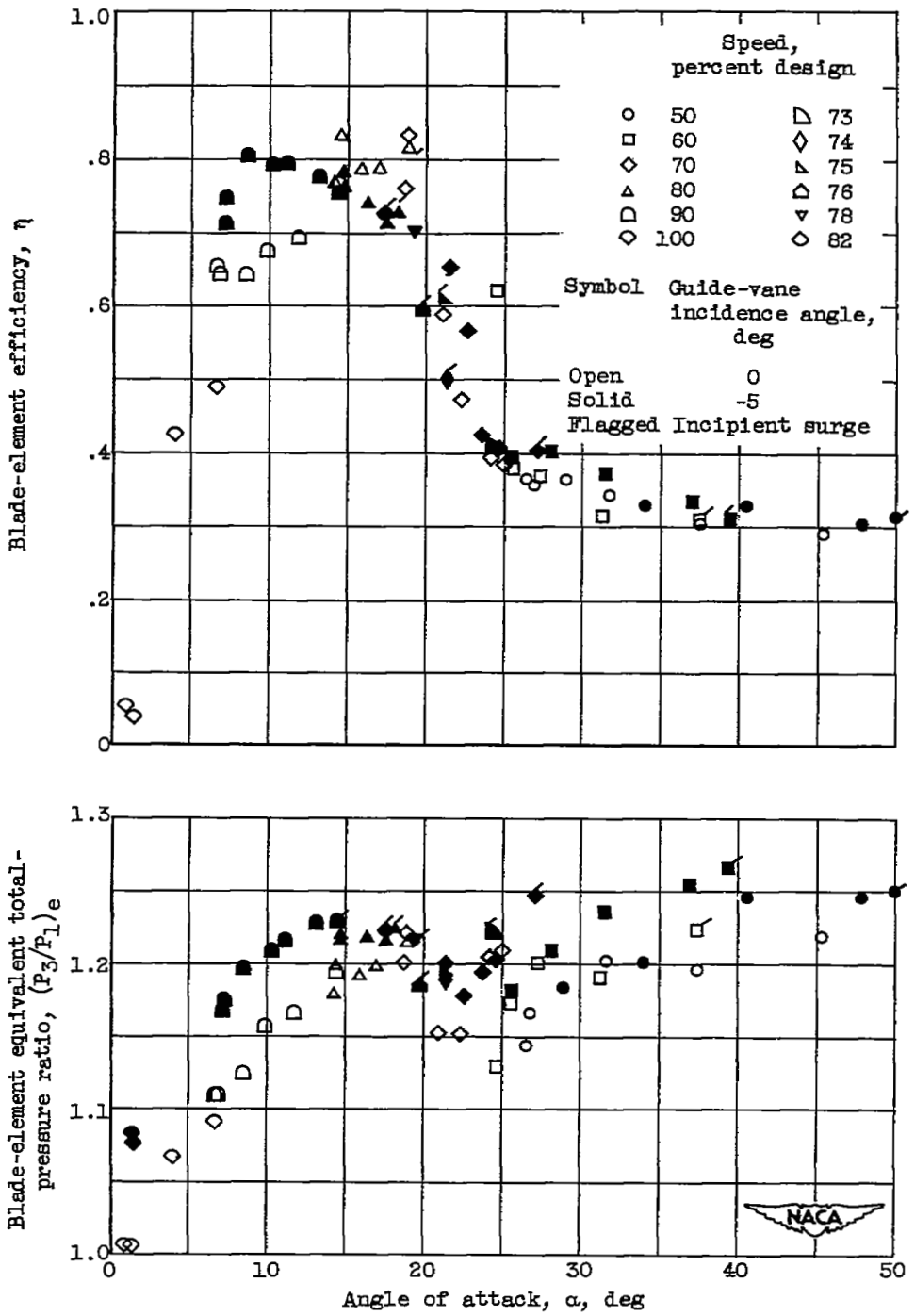

(a) Radial position a.

Figure 9. - Element performance across inlet stage at five radii over range of speed and weight flow.

[redacted]

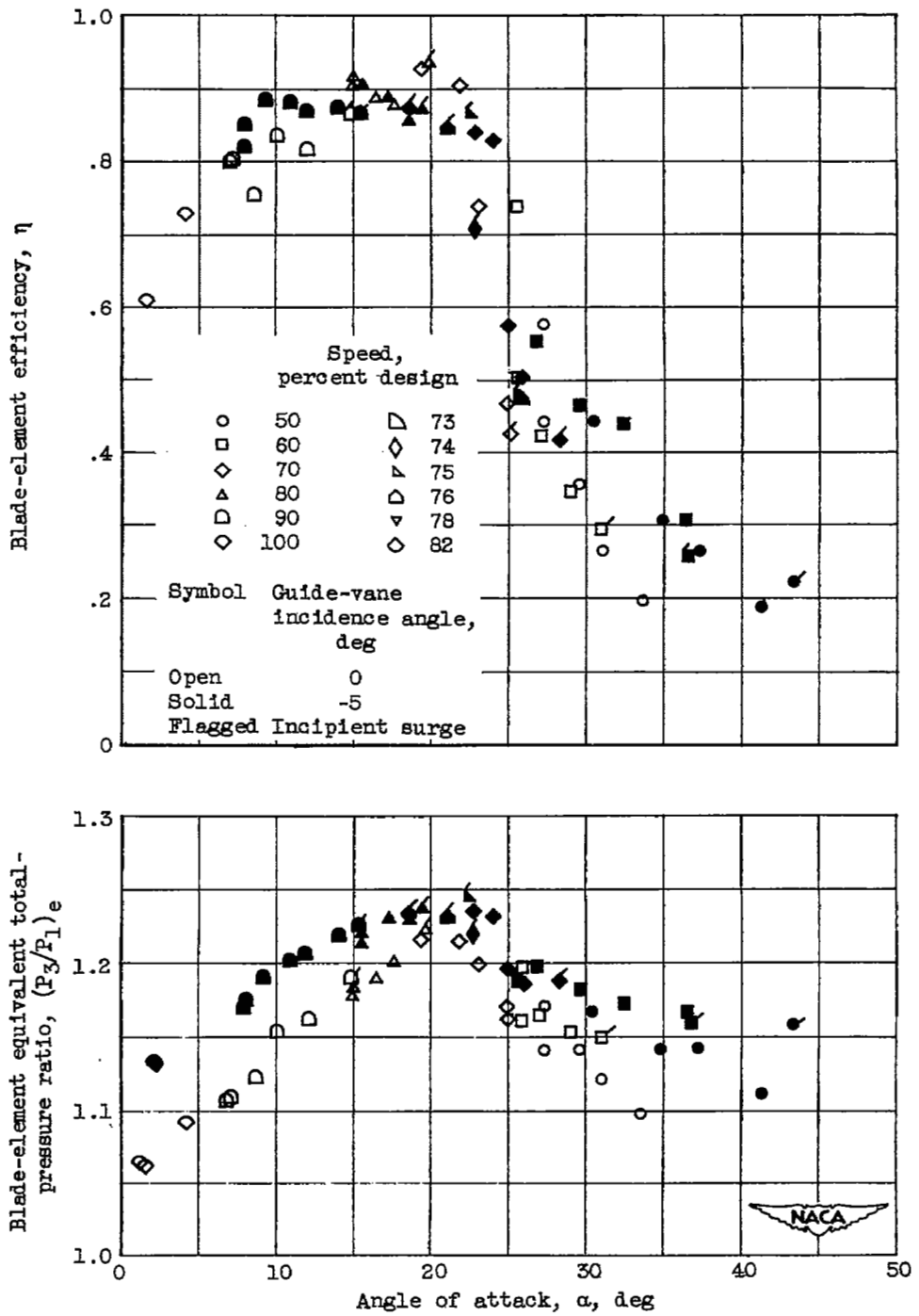

(b) Radial position b.

Figure 9. - Continued. Element performance across inlet stage at five radii over range of speed and weight flow.

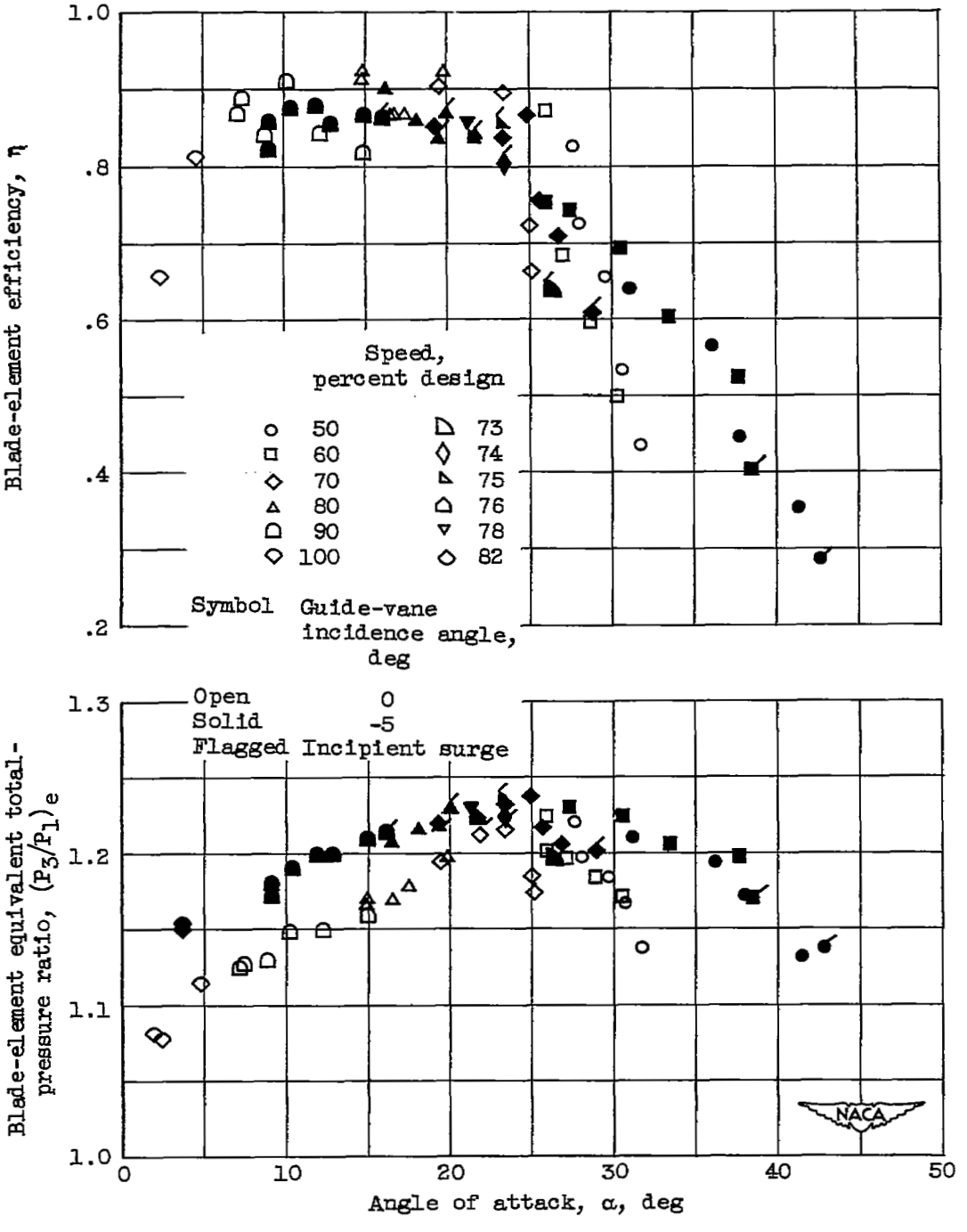

(c) Radial position c.

Figure 9. - Continued. Element performance across inlet stage at five radii over range of speed and weight flow.

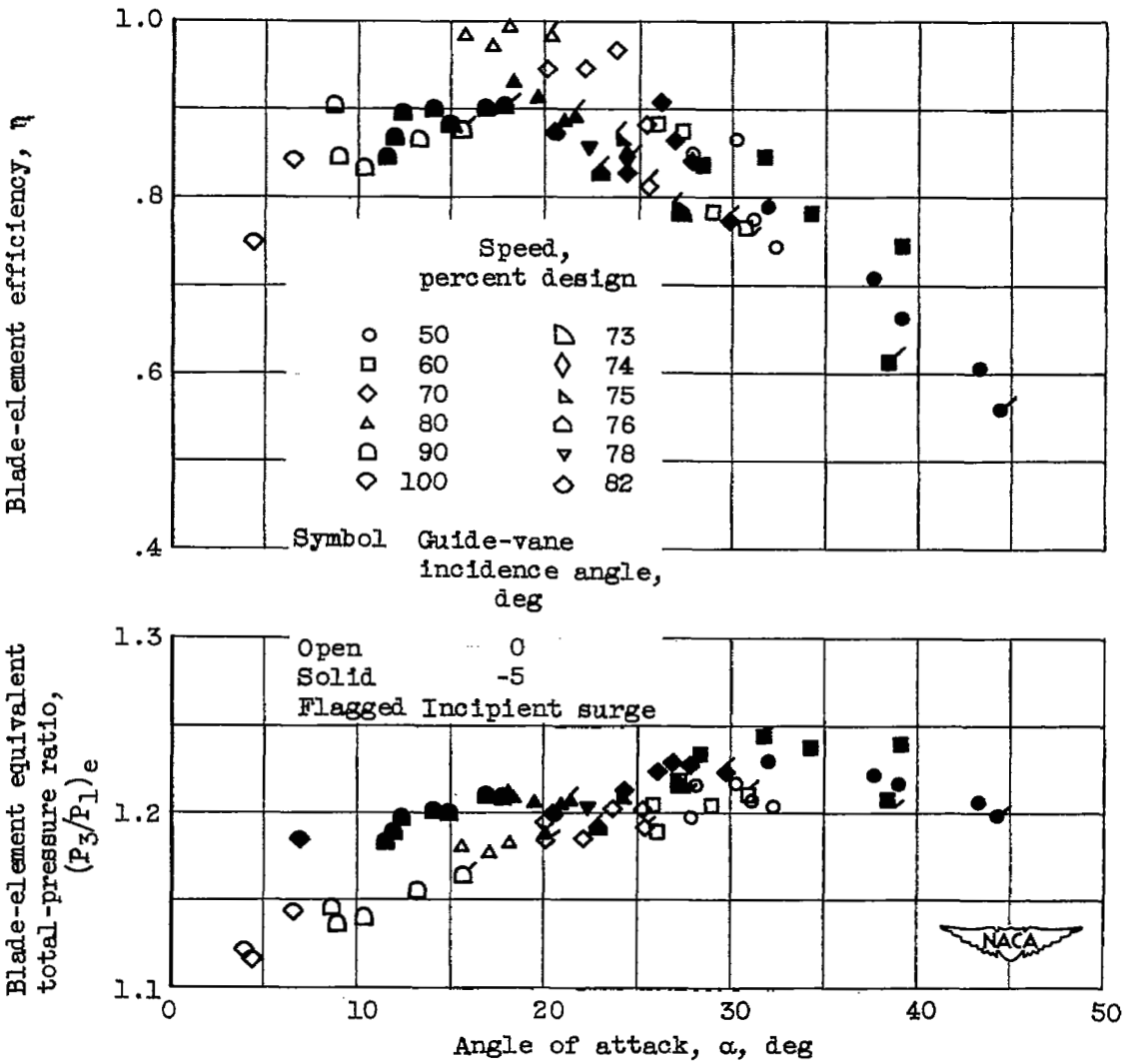

(d) Radial position d.

Figure 9. - Continued. Element performance across inlet stage at five radii over range of speed and weight flow.

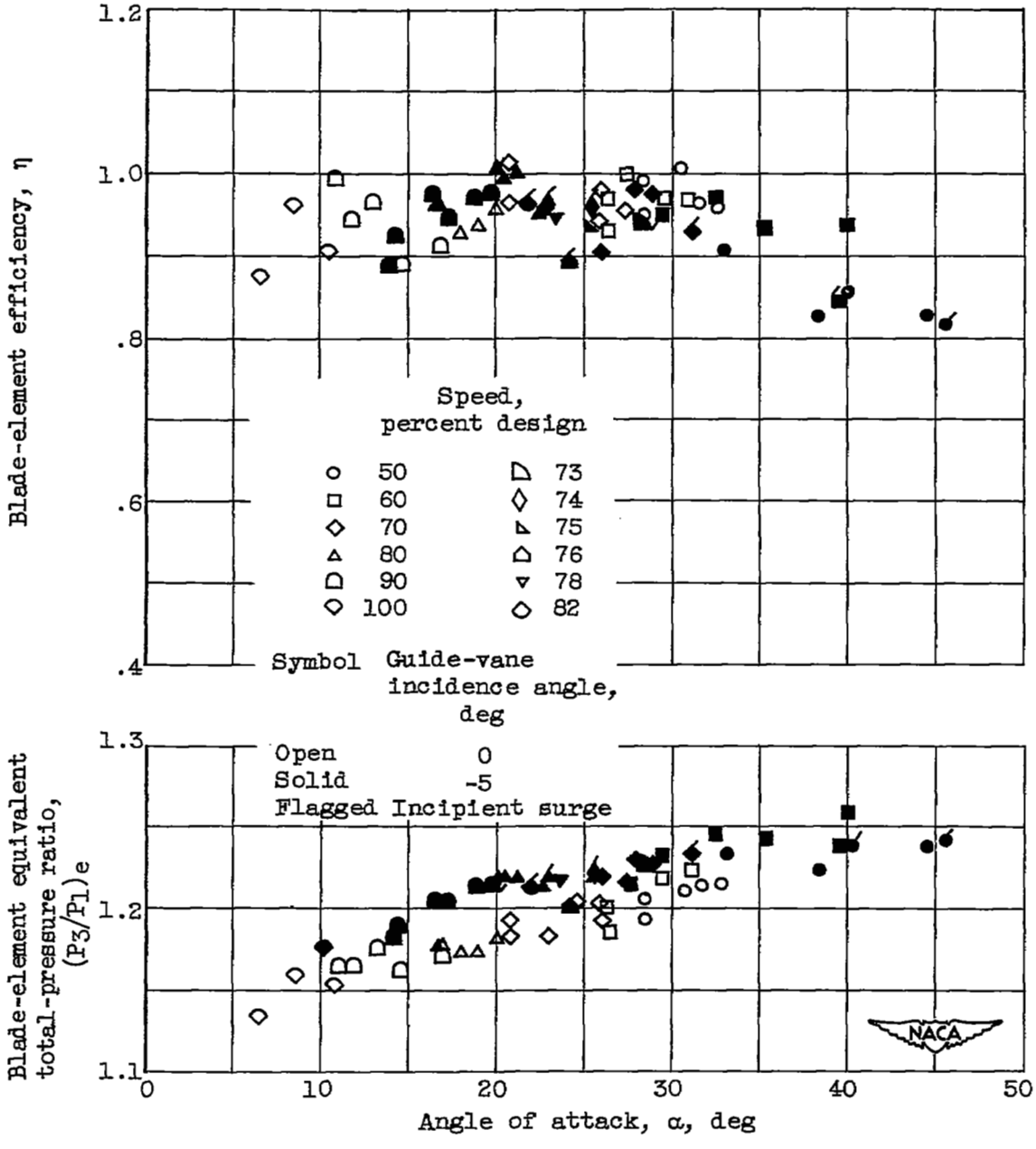

(e) Radial position e.

Figure 9. - Concluded. Element performance across inlet stage at five radii over range of speed and weight flow.

[redacted]

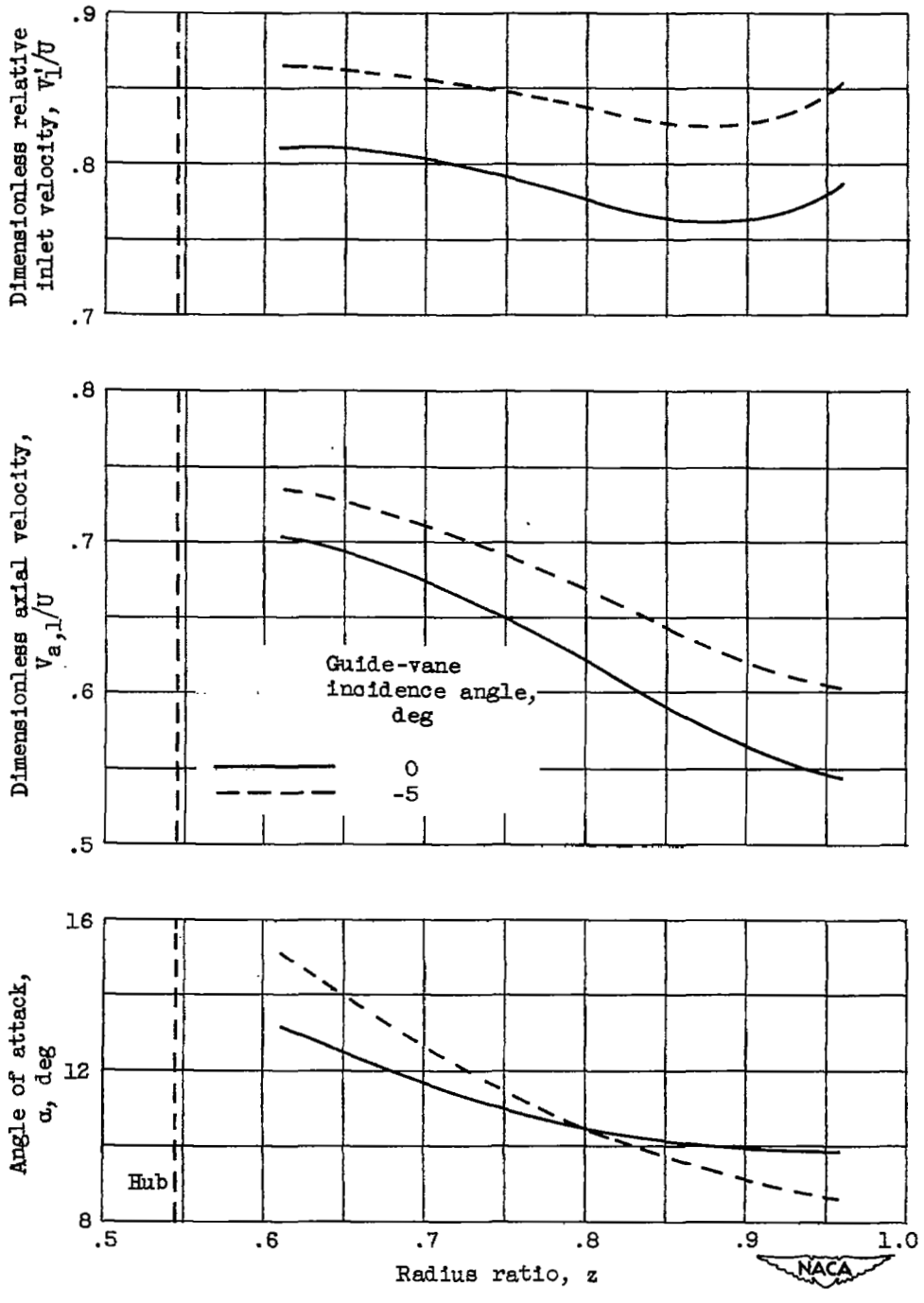

Figure 10. - Radial distribution of flow conditions entering first rotor calculated with assumption of simple radial equilibrium for same mean-radius angle of attack for both guide-vane settings.

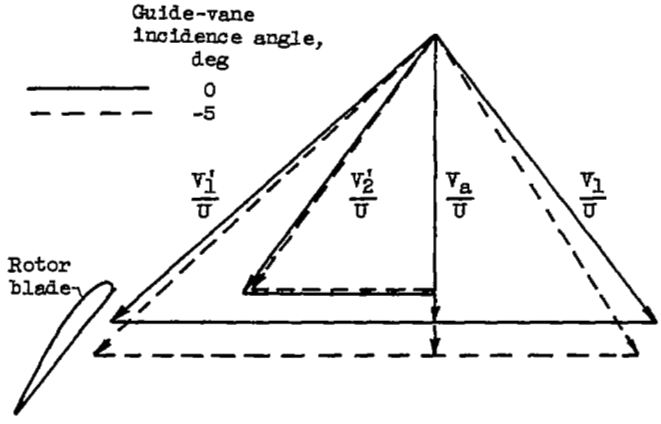

(a) Radial position a.

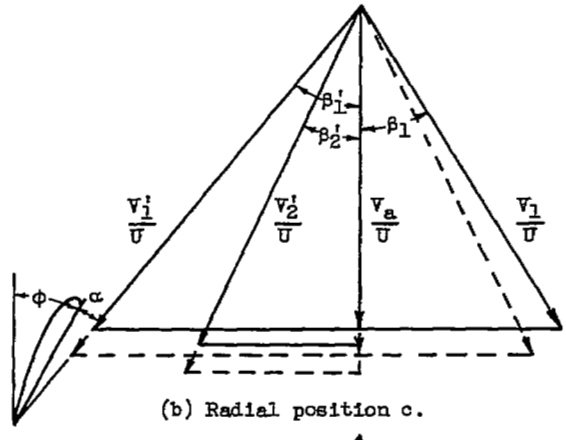

(b) Radial position c.

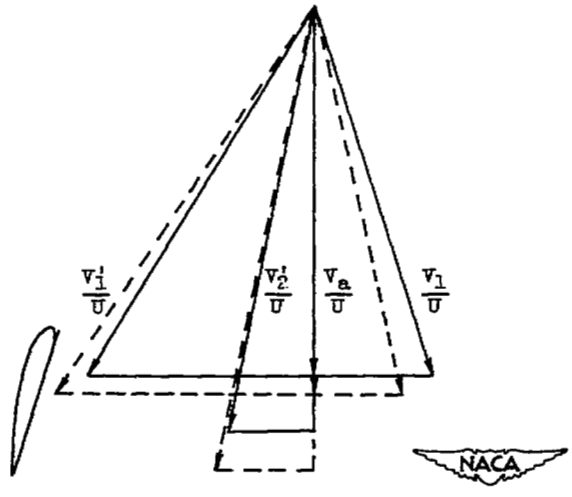

(c) Radial position e.

Figure 11. - Velocity vector diagrams at three radii for first rotor at 0° and -5° guide-vane incidence angles for same mean-radius angle of attack.

[redacted]

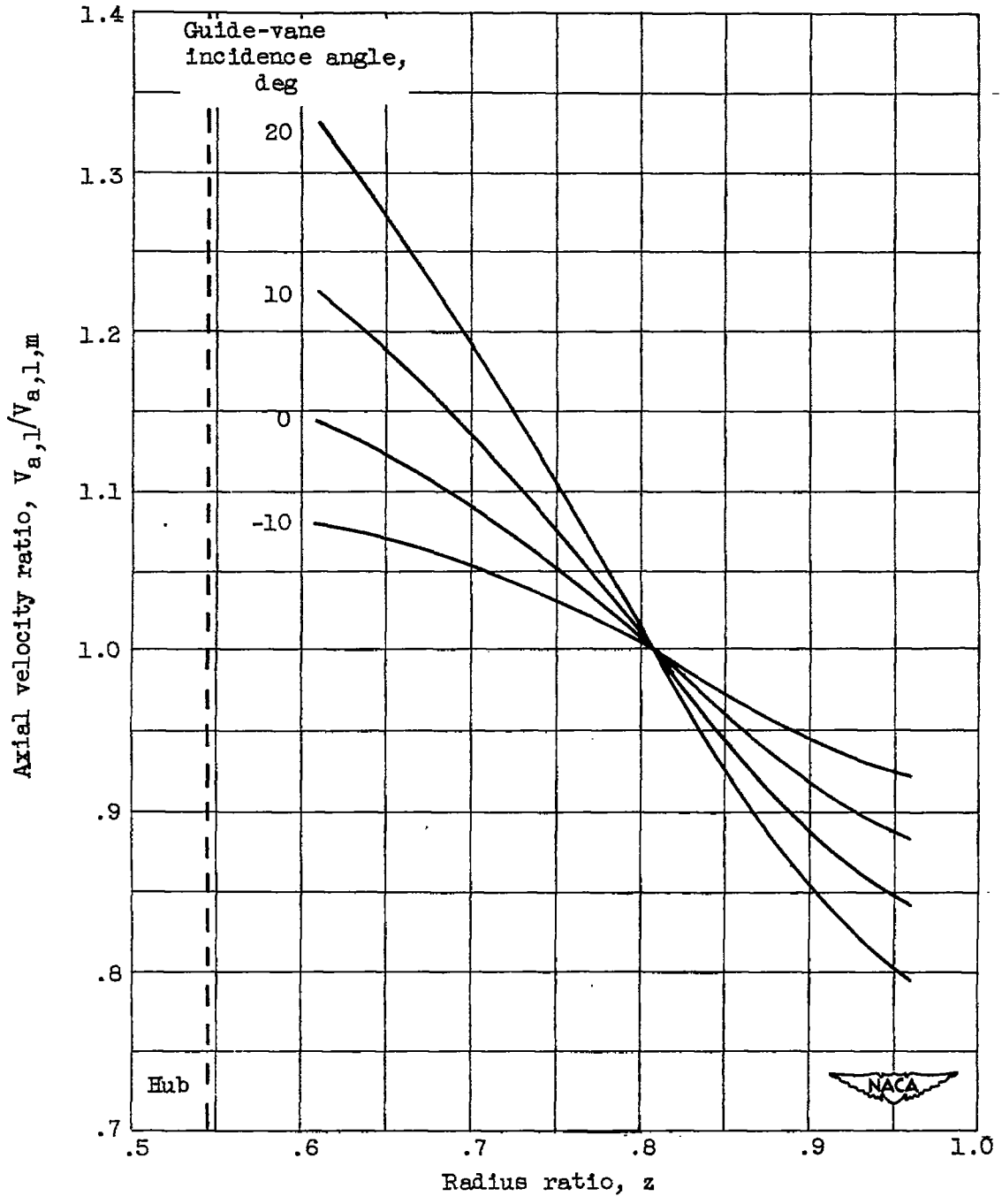

(a) Axial velocity.

Figure 12. - Radial distribution of axial velocity and angle of attack on first rotor for guide-vane incidence angles from -10° to 20°.

[redacted]

NACA-Langley - 3-15-54 - 325

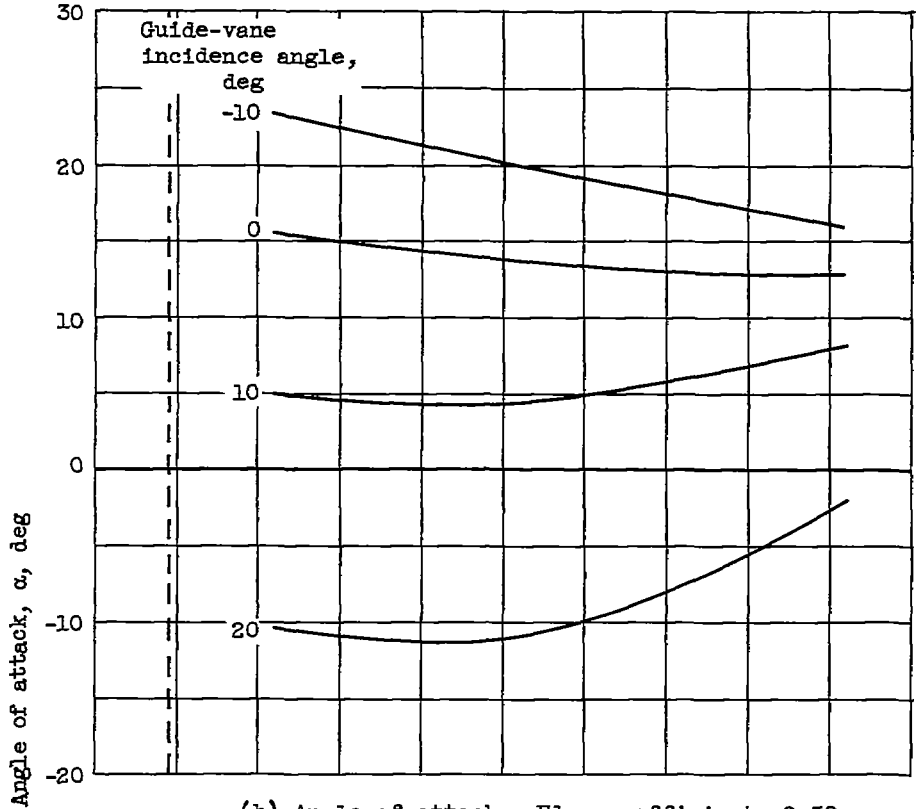

(b) Angle of attack. Flow coefficient, 0.58.

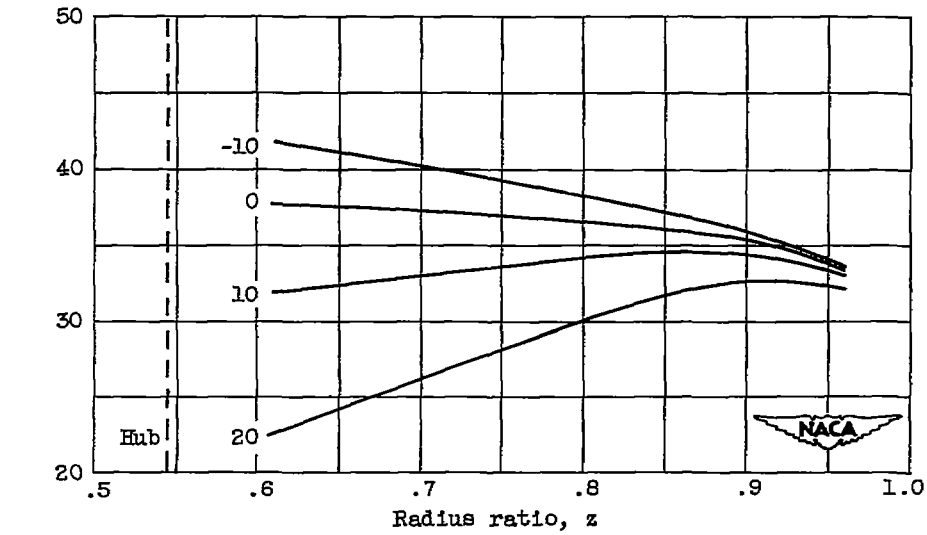

(c) Angle of attack. Flow coefficient, 0.31.

Figure 12. - Concluded. Radial distribution of axial velocity and angle of attack on first rotor for guide-vane incidence angles from -10° to 20°.

NACA-Langley - 3-15-54 - 325